Infrared Spectra of CNbO, CMO^-, OMCCO, $(C_2)MO_2$, and $M(CO)_x$ ($x = 1-6$) (M = Nb, Ta) in Solid Neon

Mingfei Zhou and Lester Andrews*

Department of Chemistry, University of Virginia, Charlottesville, Virginia 22901

Received: May 11, 1999; In Final Form: July 30, 1999

Laser ablated niobium and tantalum atoms have been reacted with CO molecules during condensation in excess neon. The $Nb(CO)_x$ and $Ta(CO)_x$ ($x = 1-6$) carbonyls formed during sample deposition or on annealing are the major products. The novel CNbO carbide−oxide molecule was produced on visible photolysis via isomerization of the NbCO carbonyl. The ONbCCO and OTaCCO molecules were formed by near-UV−vis photon-induced rearrangement of the $Nb(CO)_2$ and $Ta(CO)_2$ dicarbonyls and further rearrange to the $(C_2)NbO_2$ and $(C_2)TaO_2$ molecules on UV photolysis. Evidence is also presented for the $CNbO^-$, $CTaO^-$, $Nb(CO)_x^-$, and $Ta(CO)_x^-$ anions. The product absorptions were identified by isotopic substitution ($^{13}C^{16}O$, $^{12}C^{18}O$, and mixtures), electron trapping with added CCl_4, and density functional calculations of isotopic frequencies.

Introduction

The interaction of carbon monoxide with transition metal atoms, clusters and surfaces has been the focus of extensive and continuous study as transition metals play an important role in catalytic reactions.[1] Binary tantalum carbonyls have been prepared by reactions of tantalum atoms with CO in an argon matrix and tentatively identified by infrared spectroscopy.[2] The ground state of NbCO has also been determined by argon matrix electron spin resonance study.[3] More recently, potential energy surfaces for the low-lying electronic states of NbCO and TaCO have been studied using complete active space multi-configuration self-consistent field (CAS-MCSCF) and multireference singles + doubles configuration interaction (MRSDCI) methods.[4,5] In the gas phase, the reactivity of niobium clusters with CO has been studied experimentally and found to exhibit a strong size dependence.[6−8] Reactions of ground-state Nb^+ with CO were also investigated using guided ion beam mass spectrometry, which form NbC^+ and NbO^+ in endothermic processes.[9]

Laser ablation is an effective method of producing clean metal atoms, cations and electrons for matrix isolation study, especially for high melting point, refractory metals such as niobium and tantalum.[10,11] Co-deposition of laser-ablated transition metal atoms, cations and electrons with CO forms metal carbonyl cations and anions as well as neutral molecules for matrix infrared examination.[12−14] Comparison of product yields with and without added electron scavenger, as well as density functional calculations, makes possible the conclusive identification of cations, neutrals and anions. In this study, we report the reactions of laser-ablated niobium and tantalum atoms with CO in excess neon. We show that metal carbonyls and their corresponding anions are formed and trapped. In addition, the novel photon-induced isomization of the $M(CO)_2$ dicarbonyls to OMCCO and to $(C_2)MO_2$ molecules (M = Nb, Ta) and of NbCO to the novel metal-inserted CNbO molecule are observed.

Experimental Section

The experiment for laser ablation and matrix isolation spectroscopy has been described in detail previously.[15,16] Briefly, the Nd:YAG laser fundamental (1064 nm, 10 Hz repetition rate with 10ns pulse width) was focused on the rotating metal target (niobium, Johnson-Matthey, 99.8%; tantalum, Mackay, 99.99%). Laser-ablated metal atoms were co-deposited with carbon monoxide (0.05−0.2%) in excess neon onto a CsI cryogenic window (4 K, APD Cryogenics, Heliplex) at 2−4 mmol/h for 30−60 min. Carbon monoxide (Matheson) and isotopic $^{13}C^{16}O$ and $^{12}C^{18}O$ (Cambridge Isotopic Laboratories) and selected mixtures were used in different experiments. FTIR spectra were recorded at 0.5 cm^{-1} resolution on a Nicolet 750 spectrometer with 0.1 cm^{-1} accuracy using a HgCdTe detector. Matrix samples were annealed at different temperatures using resistance heat, and selected samples were subjected to broadband photolysis by a medium-pressure mercury arc (Philips, 175W) with the globe removed (240−580 nm).

Results and Discussion

Infrared Spectra. Experiments were done for laser-ablated Nb and Ta atom reactions with CO in neon using low laser energy ranging from 1mJ/pulse to 5mJ/pulse with different CO concentrations (0.05 to 0.2%). Typical infrared spectra in important regions are shown in Figures 1−4, and the product absorptions are listed in Tables 1 and 2. Absorptions common to these experiments, namely, CO, $(CO)_2^+$, and $(CO)_2^-$ are listed in Table 1.[13,14,17] Different temperature annealing and wavelength range photolyses were done as shown in Figures 1−4 to group product bands and to characterize the absorbing species.

Experiments were done with $^{13}C^{16}O$ and $^{12}C^{18}O$ samples, the same behavior was observed, and isotopic frequencies are also listed in Tables 1 and 2. Similar experiments with $^{12}C^{16}O+^{13}C^{16}O$ and $^{12}C^{16}O+^{12}C^{18}O$ mixtures were also performed, and diagnostic spectra are shown in Figures 5−9.

Calculations. Density functional theory calculations (DFT) were performed on simple potential product molecules to support band identification using the Gaussian 94 program.[18] Most calculations employed the BP86 functional but comparisons were done with the B3LYP functional as well.[19,20] The D95* basis set for C and O atoms and the Los Alamos ECP plus DZ for Nb and Ta atoms were used.[21,22] Calculations were first

10.1021/jp991552a CCC: $18.00
Published on Web 09/15/1999

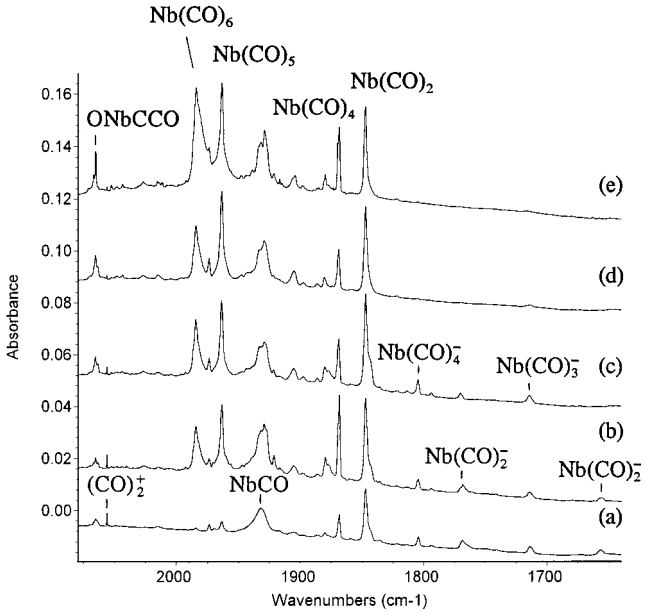

Figure 1. Infrared spectra in the 2080−1640 cm^{-1} region for laser-ablated niobium co-deposited with 0.1% CO in neon at 4 K. (a) After 30 min sample deposition, (b) after annealing to 8 K, (c) after 15 min $\lambda > 380$ nm photolysis, (d) after 15 min full-arc photolysis, and (e) after annealing to 10K.

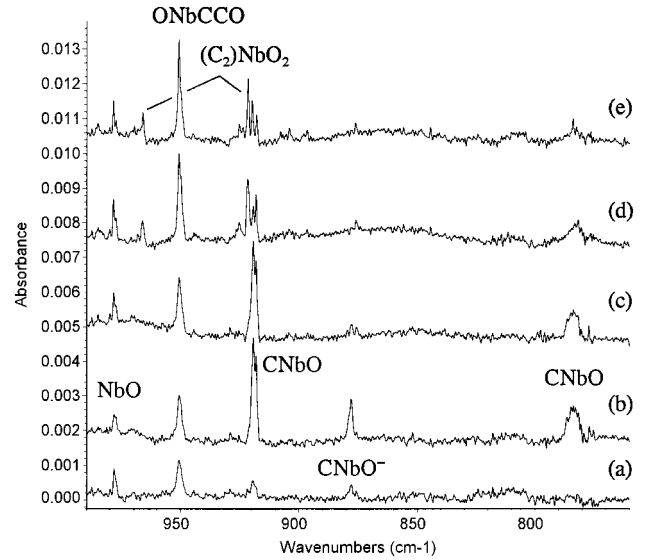

Figure 2. Infrared spectra in the 990−760 cm^{-1} region for laser-ablated Nb co-deposited with 0.2% CO in neon at 4 K. (a) After 30 min sample deposition, (b) after 15 min $\lambda > 470$ nm photolysis, (c) after 15 min $\lambda > 380$ nm photolysis, (d) after 15 min full-arc photolysis, and (f) after annealing to 10 K.

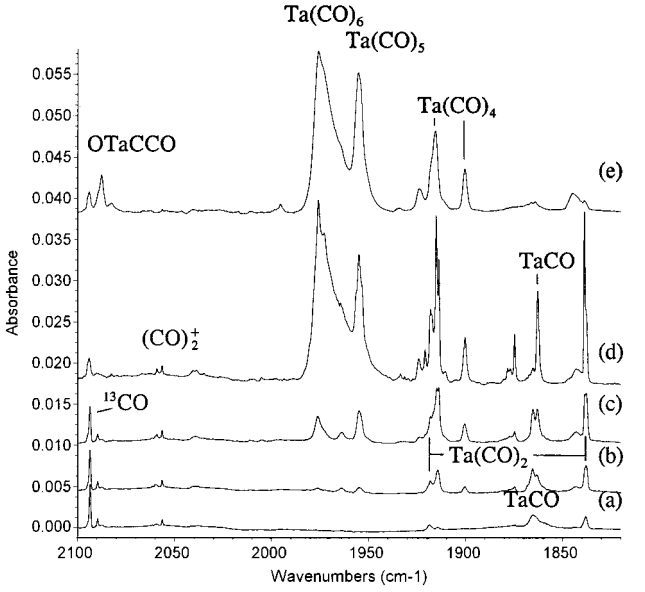

Figure 3. Infrared spectra in the 2100−1820 cm^{-1} region for laser-ablated Ta co-deposited with 0.05% CO in neon at 4 K. (a) After 30 min sample deposition, (b) after annealing to 6 K, (c) after annealing to 8 K, (d) after annealing to 10 K, and (e) after 15 min full-arc photolysis.

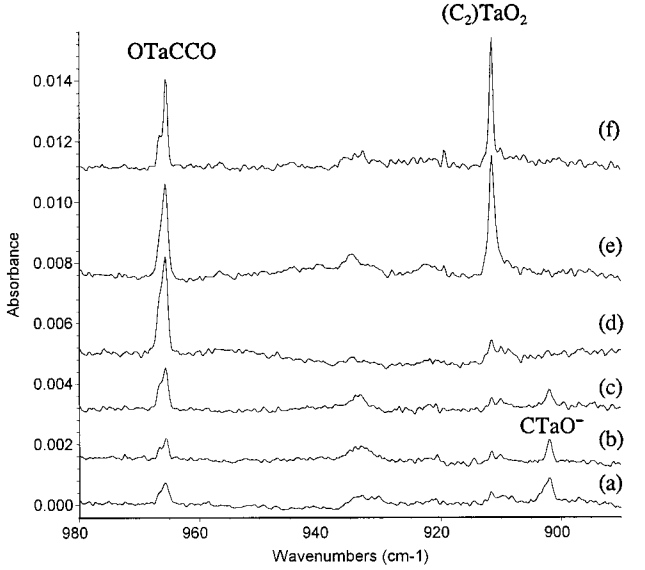

Figure 4. Infrared spectra in the 980−880 cm^{-1} region for laser-ablated Ta co-deposited with 0.1% CO in neon at 4 K. (a) After 30 min sample deposition, (b) after annealing to 6 K, (c) after 15 min $\lambda > 380$ nm photolysis, (d) after 15 min $\lambda > 290$ nm photolysis, (e) after 15 min full-arc photolysis, and (f) after annealing to 10 K.

performed on three MCO isomers, namely, carbonyl MCO, side-bonded M[CO], and inserted CMO, using both functionals, and the optimized geometries and relative energies are listed in Table 3. The BP86 functional frequency calculations are listed in Table 4; the B3LYP frequencies are 3−5% higher as expected for this hybrid functional.[23] The NbCO molecule is predicted to have a $^6\Sigma^+$ ground state using both functionals, which is in agreement with the ESR spectrum[3] and recent CASMCSCF and MRSDCI calculations.[5] For the TaCO molecule, our BP86 calculation predicted the $^6\Sigma^+$ ground state with a $^4\Delta$ state lying 1.7 kcal/mol higher in energy. On the contrary, B3LYP calculation found the $^4\Delta$ state 3.0 kcal/mol lower. A recent CASMCSCF calculation also predicted the $^6\Sigma^+$ state to be lower, whereas the MRSDCI calculation gave a $^4\Delta$ ground state.[4] Both inserted and side-bonded molecules are higher in energy than ground-state NbCO and TaCO molecules. The inserted CNbO and CTaO molecules have $^2A'$ ground states, while the side-bonded Nb[CO] and Ta[CO] molecules converged only for $^6A'$ states. Analogous calculations were also done for carbonyl and inserted anions, and the results are also listed in Tables 3 and 4.

Similar BP86 calculations were performed for three $M(CO)_2$ isomers, namely the $M(CO)_2$ dicarbonyls and the OMCCO and $(C_2)MO_2$ molecules, and the results are listed in Table 5, along with the dicarbonyl anion parameters. In addition, BP86 calculations were done for tricarbonyls and their anions in C_{3v} and C_s structures, and the results are listed in Table 6.

TABLE 1: Infrared Absorptions (cm^{-1}) from Co-Deposition of Laser-Ablated Niobium Atoms and Carbon Monoxide Molecules in Excess Neon

$^{12}C^{16}O$	$^{13}C^{16}O$	$^{12}C^{18}O$	$^{12}C^{16}O+^{13}C^{16}O$	$^{12}C^{16}O+^{12}C^{18}O$	$R(^{12}C/^{13}C)$	$R(^{16}O/^{18}O)$	assignment
2140.8	2093.6	2089.7	2140.8, 2093.6	2140.8, 2089.8	1.0225	1.0245	CO
2065.5	2005.0	2039.7	2065.6, 2058.8, 2013.2, 2005.1	2065.6, 2039.8	1.0302	1.0126	ONbCCO
2056.3	2010.9	2007.4	2056.4, 2018.4, 2010.9	2056.3, 2016.4, 2007.4	1.0226	1.0244	$(CO)_2$+
1984.1	1940.7	1936.6			1.0224	1.0245	$Nb(CO)_6$
1973.6	1927.9	1930.4			1.0237	1.0224	
1963.5	1920.8	1916.5			1.0222	1.0245	$Nb(CO)_5$
1932.0	1887.9	1887.6	1931.9, 1888.1	1932.0, 1887.6	1.0234	1.0235	NbCO
1929.1	1886.6	1882.4			1.0225	1.0248	$(Nb(CO)_3)$
1904.1	1861.7	1859.9			1.0228	1.0238	$(Nb(CO)_3)$
1879.9	1837.8	1836.4			1.0229	1.0237	$Nb_x(CO)_y$?
1868.3	1827.8	1823.1	1868.3, 1853.0, 1841.1, 1834.8, 1827.8	1868.5, 1851.7, 1838.8, 1830.3, 1823.3	1.0222	1.0248	$Nb(CO)_4$
1847.2	1805.6	1804.9	1847.1, 1821.5, 1805.6	1846.9, 1821.1, 1804.6	1.0230	1.0234	$Nb(CO)_2$
1804.3	1764.5	1761.7			1.0226	1.0242	$Nb(CO)_4^-$
1793.7	1751.8	1754.0			1.0239	1.0226	$Nb(CO)_3^-$
1768.6	1728.1	1730.6	1768.6, 1751.5, 1728.1	1768.6, 1761.5, 1730.6	1.0234	1.0220	$Nb(CO)_2^-$
1713.7	1673.8	1676.2	1713.6, 1696.3, 1684.0, 1673.2	1713.5, 1698.0, 1686.6, 1676.1	1.0238	1.0224	$Nb(CO)_3^-$
1656.7	1619.4	1618.9	1656.7, 1634.1, 1619.4		1.0230	1.0233	$Nb(CO)_2^-$
1517.4	1484.2	1481.2	1517.4, 1499.4, 1484.2	1517.4, 1499.3, 1481.2	1.0224	1.0244	$(CO)_2^-$
1516.3	1483.0	1490.4	1516.3, 1498.1, 1483.0	1516.2, 1498.3, 1490.4	1.0225	1.0243	$(CO)_2^-$
978.6	978.6	931.2		978.6, 931.2		1.0509	NbO
966.2	966.2	918.1		966.2, 952.0, 918.0		1.0524	$(C_2)NbO_2$
950.9	950.9	904.9		950.8, 905.0		1.0508	ONbCCO
921.6	921.6	879.2		921.6, 890.6, 879.2		1.0490	$(C_2)NbO_2$
919.8	915.9	883.1	919.8, 915.8	919.8, 883.1	1.0043	1.0416	CNbO
918.0	914.1	881.5	918.0, 914.1	918.0, 881.5	1.0043	1.0414	CNbO site
877.8	875.0	840.7	877.8, 875.0	877.8, 840.5	1.0032	1.0441	$CNbO^-$
783.7	760.2	777.1	783.7, 760.2	783.8, 777.1	1.0309	1.0085	CNbO
782.4	759.0	776.0			1.0308	1.0082	CNbO site

TABLE 2: Infrared Absorptions (cm^{-1}) from Co-Deposition of Laser-Ablated Tantalum Atoms and Carbon Monoxide in Excess Neon

$^{12}C^{16}O$	$^{13}C^{16}O$	$^{12}C^{18}O$	$^{12}C^{16}O+^{13}C^{16}O$	$^{12}C^{16}O+^{12}C^{18}O$	$R(^{12}C/^{13}C)$	$R(^{16}O/^{18}O)$	assignment
2087.5	2026.2	2061.6	2087.5, 2080.0, 2037.5, 2026.3	2087.5, 2061.6	1.0303	1.0126	OTaCCO
2017.2	1973.1	1969.0			1.0224	1.0245	$Ta(CO)_x$
1995.3	1949.6	1949.3			1.0234	1.0236	$Ta(CO)_x$
1976.0	1932.7	1928.8			1.0224	1.0245	$Ta(CO)_6$
1954.7	1912.0	1908.1			1.0223	1.0244	$Ta(CO)_5$
1918.3	1874.3	1876.6	1918.5, 1901.7, 1874.3	1918.3, 1902.6, 1876.7	1.0235	1.0222	$Ta(CO)_2$
1915.2	1873.5	1869.4			1.0223	1.0245	$Ta(CO)_4$
1900.1	1857.3	1856.7			1.0230	1.0234	$Ta(CO)_4$
1874.6	1833.8	1829.6	1874.6, 1848.4, 1833.8		1.0222	1.0246	$(Ta(CO)_3)$
1865.2	1825.2	1821.5	1865.1, 1825.2	1865.2, 1821.4	1.0219	1.0240	TaCO
1862.7	1822.9	1819.9	1862.8, 1823.0		1.0218	1.0235	TaCO
1838.6	1796.6	1797.2	1838.6, 1812.2, 1796.8	1838.3, 1812.5, 1796.3	1.0234	1.0230	$Ta(CO)_2$
1799.5	1759.3	1757.8			1.0228	1.0237	$(Ta(CO)_4^-)$
1794.3	1752.6	1755.0			1.0238	1.0224	$(Ta(CO)_3^-)$
1773.6	1732.3	1735.2			1.0238	1.0221	$(Ta(CO)_2^-)$
1716.4	1675.2	1680.5			1.0246	1.0213	$(Ta(CO)_3^-)$
1700.9	1663.4				1.0225		$(TaCO^-)$
1020.0	1020.0	966.8		1020.0, 966.8		1.0550	TaO
965.7	965.7	915.5		965.7, 915.5		1.0548	OTaCCO
911.5	911.5	865.2		949.5, 911.6, 878.7, 865.3		1.0535	$(C_2)TaO_2$
902.0	900.3	857.7		902.0, 857.7	1.0019	1.0516	$CTaO^-$
884.2	884.2	839.3		884.2, 853.8, 839.3		1.0535	$(C_2)TaO_2(CO)_x$
864.3	864.3	821.3		864.3, 832.8, 821.3		1.0524	$(C_2)TaO_2(CO)_x$

Finally, similar calculations were done for dimetal dicarbonyl species in bridged and terminal carbonyl structures. For both Nb and Ta, the bridged (^1A_g) rhombic structure $OC(M)_2CO$ is more stable (by 30−40 kcal/mol) than the trans and cis OCMMCO forms. The rhombic structures give very strong bridged carbonyl bands (b_u) at 1731 and 1689 cm^{-1} for the Nb and Ta species, respectively, which are not observed here as bands in this region are due to anions based on the CCl_4 doping behavior discussed below.

$Nb(CO)_x$ ($x = 1-6$). Laser-ablated niobium atoms react with carbon monoxide in excess neon during condensation to form primarily $Nb(CO)_x$ species identified here for the first time using a factor of 10 lower laser power compared to previous experiments with dioxygen in excess argon.[10] With a reactive molecule like CO and a low concentration of metal atoms (estimated <0.1%), molecules with more than one metal atom are unlikely to be major products. Even with higher laser power, possible dimetal species are minor contributors to the dioxygen product spectrum.[10] In contrast, previous experiments with Y, La and N_2 gave $(YN)_2$ and $(LaN)_2$ species where the *much lower* reactivity of N_2 and *very small* concentration of N atoms markedly increase the probability of a secondary metal atom reaction.[24] The present experiments vary the laser power (and approximately the metal atom concentration) over a 5-fold range, and the family of bands assigned to $Nb(CO)_x$ species maintain constant relative intensities, which is consistent with a common low Nb stoichiometry. Excellent agreement between observed and BP86 calculated frequencies, which have a proven track

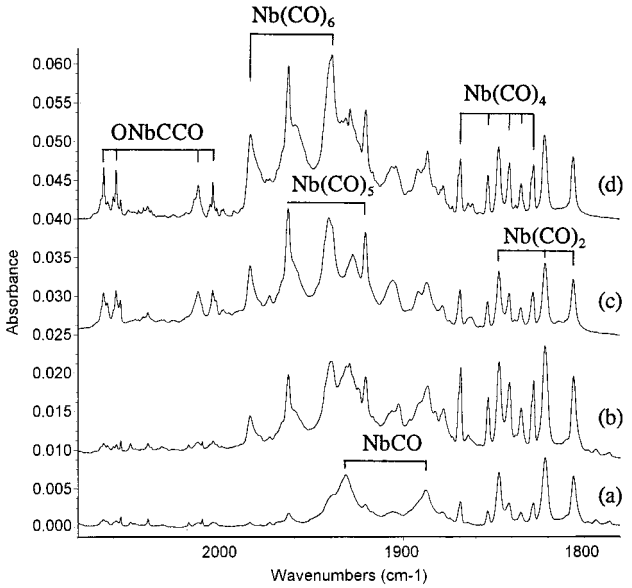

Figure 5. Infrared spectra in the 2080−1780 cm^{-1} region for laser-ablated Nb co-deposited with 0.1%$^{12}C^{16}O$+0.1%$^{13}C^{16}O$ in neon at 4 K. (a) After 45 min sample deposition, (b) after annealing to 8 K, (c) after 15 min full-arc photolysis, and (d) after annealing to 10 K.

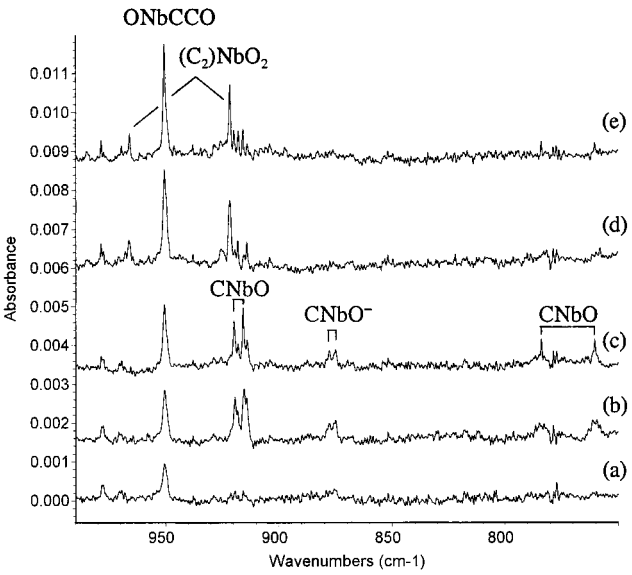

Figure 6. Infrared spectra in the 990−750 cm^{-1} region for laser-ablated Nb co-deposited with 0.1%$^{12}C^{16}O$+0.1%$^{13}C^{16}O$ in neon at 4 K. (a) After 45 min sample deposition, (b) after 15 min $\lambda > 470$ nm photolysis, (c) after annealing to 8 K, (d) after 15 min full-arc photolysis, and (e) after annealing to 10 K.

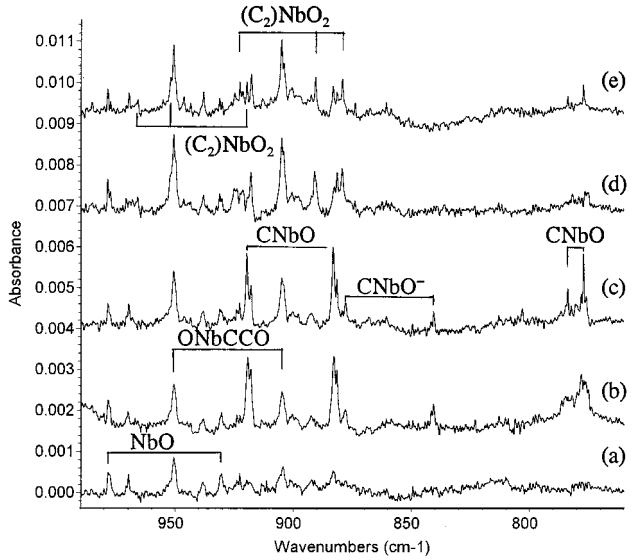

Figure 7. Infrared spectra in the 990−750 cm^{-1} region for laser-ablated Nb co-deposited with 0.1%$^{12}C^{16}O$+0.1%$^{12}C^{18}O$ in neon at 4 K, (a) after 45 min sample deposition, (b) after 15 min $\lambda > 470$ nm photolysis, (c) after annealing to 8 K, (d) after 15 min full-arc photolysis, and (e) after annealing to 10 K.

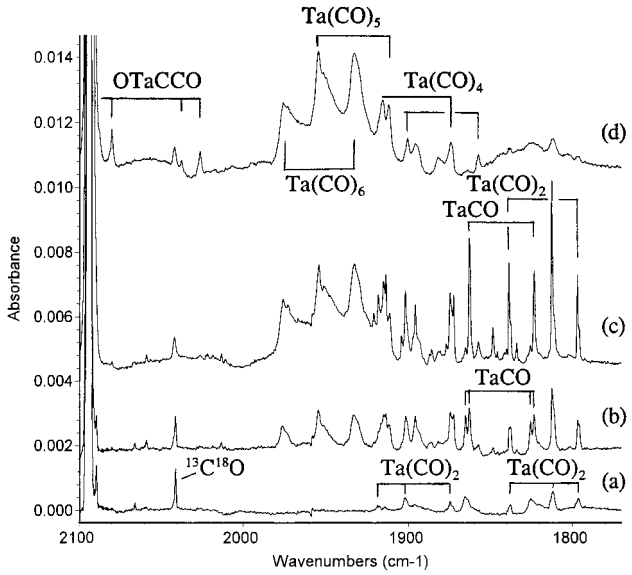

Figure 8. Infrared spectra in the 2100−1770 cm^{-1} region for laser-ablated Ta co-deposited with 0.05%$^{12}C^{16}O$+0.05%$^{13}C^{16}O$ in neon at 4 K, (a) after 45 min sample deposition, (b) after annealing to 6 K, (c) after annealing to 10 K, (d) after 15 min full-arc photolysis.

record,[12−14] shows that the major products assigned here are single metal species. We cannot rule out the possibility of dimetal species contributing minor weak unassigned absorptions.

The 1932.0 cm^{-1} band is assigned to the C−O stretching vibration of the NbCO molecule. This band appears on deposition, increases slightly on annealing, and *decreases* on visible photolysis, when absorptions at 919.8 and 783.7 cm^{-1} due to CNbO greatly *increase*. The $^{13}C^{16}O$ and $^{12}C^{18}O$ counterparts at 1887.9 and 1887.6 cm^{-1} define the 12/13 ratio 1.0234 and the 16/18 ratio 1.0235. In the mixed $^{12}C^{16}O$+$^{13}C^{16}O$ experiment, only pure isotopic counterparts are observed, which confirms the involvement of one CO submolecule in this vibrational mode. Our DFT calculations predict a C−O stretching vibration at 1916.2 cm^{-1} for NbCO with calculated isotopic frequency ratios (Table 4) in excellent agreement with observed values (scaled isotopic frequencies within ±0.6 cm^{-1}). The earlier CASMCSCF and MRSDCI calculations gave a much higher C−O stretching frequency (2133, 2135 cm^{-1}) for $^6\Sigma^+$ NbCO[5] because not enough C and O orbitals were included in the active space to accurately describe the C−O stretch.

The 1847.2 cm^{-1} absorption observed on deposition increases on annealing. In the mixed $^{12}C^{16}O$+$^{13}C^{16}O$ and $^{12}C^{16}O$+$^{12}C^{18}O$ experiments, triplet absorptions with approximately 1/2/1 relative intensities are observed, which demonstrate that two equivalent CO submolecules are involved in this vibration. Accordingly, the band is assigned to the antisymmetric C−O vibration of the $Nb(CO)_2$ molecule. Our DFT calculation predicts a $^4B_2$ ground state for the $Nb(CO)_2$ molecule. The antisymmetric C−O stretching vibration is calculated at 1852.7 cm^{-1} and the symmetric C−O stretching vibration at 1917.6 cm^{-1} with about 50% of the antisymmetric vibration intensity; however, no

TABLE 3: Geometries and Relative Energies (kcal/mol) Calculated for MCO, CMO, MCO^-, and CMO^- (M = Nb, Ta) with BP86 and B3LYP Functionals

	molecule	state	energy	geometry
BP86	NbCO	$^6\Sigma^+$	0	Nb−C: 2.064 Å, C−O: 1.182 Å, linear
		$^4\Phi$	+8.9	Nb−C: 1.966 Å, C−O: 1.199 Å, linear
	Nb[CO]	$^6A'$	+27.7	Nb−C: 2.198 Å, Nb−O: 2.337 Å, C−O: 1.216 Å
	CNbO	$^2A'$	+20.4	Nb−C: 1.826 Å, Nb−O: 1.744 Å, ∠CNbO: 102.2°
		$^4A'$	+34.3	Nb−C: 1.906 Å, Nb−O: 1.731 Å, ∠CNbO: 100.1°
	$NbCO^-$	$^5\Sigma^+$	−14.6	Nb−C: 2.064 Å, C−O: 1.203 Å, linear
		$^3\Phi$	−14.9	Nb−C: 1.954 Å, C−O: 1.221 Å, linear
	$CNbO^-$	$^3A'$	−19.6	Nb−C: 1.868 Å, Nb−O: 1.769 Å, ∠CNbO: 101.9°
	TaCO	$^4\Delta$	0	Ta−C: 2.012 Å, C−O: 1.184 Å, linear
		$^6\Sigma^+$	−1.7	Ta−C: 2.033 Å, C−O: 1.187 Å, linear
	CTaO	$^2A'$	+9.7	Ta−C: 1.922 Å, Ta−O: 1.724 Å, ∠CTaO: 101.5°
		$^4A'$	+9.9	Ta−C: 1.895 Å, Ta−O: 1.725 Å, ∠CTaO: 101.4°
	Ta[CO]	$^6A'$	+27.4	Ta−C: 2.114 Å, Ta−O: 2.381 Å, C−O: 1.229 Å
	$TaCO^-$	$^3\Phi$	−31.0	Ta−C: 1.951 Å, C−O: 1.230 Å, linear
		$^5\Sigma^+$	−25.5	Ta−C: 2.049 Å, C−O: 1.210 Å, linear
	$CTaO^-$	$^3A'$	−44.9	Ta−C: 1.909 Å, Ta−O: 1.757 Å, ∠CTaO: 103.8 Å
B3LYP	NbCO	$^6\Sigma^+$	0	Nb−C: 2.080 Å, C−O: 1.168 Å, linear
		$^4\Phi$	+7.8	Nb−C: 1.985 Å, C−O: 1.182 Å, linear
	Nb[CO]	$^6A'$	+25.6	Nb−C: 2.247 Å,Nb−O: 2.347 Å, C−O: 1.196 Å
	CNbO	$^2A'$	+29.1	Nb−C: 1.820 Å, Nb−O: 1.733 Å, ∠CNbO: 102.6°
		$^4A'$	+42.3	Nb−C: 1.907 Å, Nb−O: 1.719 Å, ∠CNbO: 100.9°
	$NbCO^-$	$^5\Sigma^+$	−14.2	Nb−C: 2.069 Å, C−O: 1.190 Å, linear
		$^3\Phi$	−14.0	Nb−C: 1.965 Å, C−O: 1.206 Å, linear
	$CNbO^-$	$^3A'$	−8.5	Nb−C: 1.854 Å, Nb−O: 1.761 Å, ∠CNbO: 103.0°
	TaCO	$^4\Delta$	0	Ta−C: 2.022 Å, C−O: 1.170 Å, linear
		$^6\Sigma^+$	+3.0	Ta−C: 2.039 Å, C−O: 1.175 Å, linear
	CTaO	$^2A'$	+19.1	Ta−C: 1.923 Å, Ta−O: 1.714 Å, ∠CTaO: 102.6°
		$^4A'$	+19.2	Ta−C: 1.895 Å, Ta−O: 1.715 Å, ∠CTaO: 102.4°
	Ta[CO]	$^6A'$	+32.8	Ta−C: 2.134 Å, Ta−O: 2.387 Å, C−O: 1.212 Å
	$TaCO^-$	$^3\Phi$	−24.9	Ta−C: 1.955 Å, C−O: 1.217 Å, linear
		$^5\Sigma^+$	−18.8	Ta−C: 2.048 Å, C−O: 1.200 Å, linear
	$CTaO^-$	$^3A'$	−31.8	Ta−C: 1.906 Å, Ta−O: 1.749 Å, ∠CTaO: 105.4°

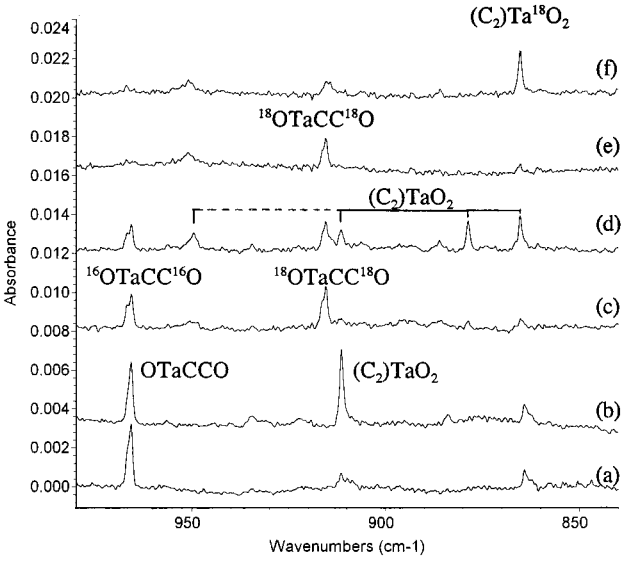

Figure 9. Infrared spectra in the 980−840 cm^{-1} region for laser ablated Ta co-deposited with isotopic CO sample in excess neon. (a) 0.1%$^{12}C^{16}O$, 15 min λ > 290 nm photolysis; (b) 0.1%$^{12}C^{16}O$, 15 min full-arc photolysis; (c) 0.1%$^{12}C^{16}O$+$^{12}C^{18}O$, 15 min λ > 290 nm photolysis; (d) 0.1%$^{12}C^{16}O$+$^{12}C^{18}O$, 15 min full-arc photolysis; (e) 0.1%$^{12}C^{18}O$, 15 min λ > 290 nm photolysis; and (f) 0.1%$^{12}C^{18}O$, 15 min full-arc photolysis.

absorption can be assigned to the symmetric mode. One possibility is that the $Nb(CO)_2$ molecule in neon has a larger bond angle and a weaker symmetric C−O stretching vibration than calculated. However, the symmetric stretching mode could easily be covered by the broad NbCO absorption centered at 1932.0 cm^{-1}; the shoulder at 1934 cm^{-1} that grows on annealing could be due to the symmetric stretching mode of $Nb(CO)_2$. Finally, both $V(CO)_2$ and $Ta(CO)_2$ are bent molecules with observed symmetric and antisymmetric C−O stretching modes,[25] a fact which suggests that $Nb(CO)_2$ is also bent.

Figure 1 shows that the 1932.0 cm^{-1} NbCO and 1847 cm^{-1} $Nb(CO)_2$ bands both increase on annealing to 8 K. The 1847.2 cm^{-1} band is sharp in all spectra, and it is unlikely that any secondary metal atoms are involved to give a weakly bonded Nb−$Nb(CO)_2$ type of species. However, the 1932.0 cm^{-1} band develops shoulders on annealing and the possible contribution of a metal-perturbed species such as Nb−NbCO cannot be ruled out. Clearly a bridged $(Nb)_2CO$ species, expected to be more stable from our $(Nb)_2(CO)_2$ calculations, can be ruled out from the band position.

The $Nb(CO)_3$ molecule is calculated to have a $^2A_1$ ground state, C_{3v} symmetry, and a strong antisymmetric C−O stretching vibration at 1826.8 cm^{-1}. However, no band in this region can be assigned to $Nb(CO)_3$. However, a slightly higher $^4A''$ state with C_s symmetry has a strong mode calculated at 1902.7 cm^{-1} and a weaker band at 1895.3 cm^{-1}. Weak 1929.1, 1904.1 cm^{-1} bands increase in intensity together on annealing after the $Nb(CO)_2$ band, and these bands are tentatively assigned to $Nb(CO)_3$ with this lower symmetry structure. Note that bent $^4B_2$ $Nb(CO)_2$ can easily add CO on annealing to form the $^4A''$ C_s structure.

The 1868.3 cm^{-1} absorption increases on annealing after to the $Nb(CO)_2$ absorption. This band shifts to 1827.8 and 1823.1 cm^{-1} using $^{13}C^{16}O$ and $^{12}C^{18}O$ samples. In the mixed $^{12}C^{16}O$+$^{13}C^{16}O$ experiment, a quintet is produced (Figure 5) which is characteristic of the triply degenerate vibration of a tetrahedral molecule.[26] Accordingly, this band is assigned to the $Nb(CO)_4$ molecule.

TABLE 4: Isotopic "Harmonic" Frequencies (cm^{-1}), Intensities (km/mol), and Isotopic Frequency Ratios Calculated for the Structures Described in Table 3 Using the BP86 Functional

molecule	$^{12}C^{16}O$	$^{13}C^{16}O$	$^{12}C^{18}O$	$R(^{12}C^{16}O/^{13}C^{16}O)$	$R(^{12}C^{16}O/^{12}C^{18}O)$
NbCO ($^6\Sigma^+$)	1916.2(727)	1871.8(691)	1872.7(699)	1.0237	1.0232
	431.9(3)	426.5(3)	420.0(2)	1.0127	1.0283
	294.9 (4)	286.1(3)	291.1(4)	1.0308	1.0131
NbCO ($^4\Phi$)	1831.1(657)	1787.8(625)	1790.8(631)	1.0242	1.0225
	496.9(1)	490.9(1)	482.9(1)	1.0122	1.0290
	361.7(16)	350.9(15)	357.2(16)	1.0308	1.0126
	325.2(4)	315.4(4)	321.1(5)	1.0311	1.0128
Nb[CO] (^{6}A′)	1661.9(314)	1625.1(302)	1621.5(297)	1.0226	1.0249
	409.0(16)	394.9(15)	408.6(16)	1.0357	1.0010
	240.4(8)	239.9(8)	229.2(7)	1.0021	1.0489
CNbO (^{2}A′)	930.8(66)	925.2(75)	897.5(43)	1.0061	1.0371
	822.9(51)	799.1(41)	811.9(65)	1.0298	1.0135
	303.9(7)	298.0(7)	297.2(7)	1.0198	1.0225
CNbO (^{4}A′)	943.1(100)	941.7(102)	899.8(89)	1.0015	1.0481
	767.6(39)	742.4(36)	765.3(41)	1.0339	1.0030
	288.4(0.2)	283.0(0.3)	281.8(0.1)	1.0191	1.0234
$NbCO^-$ ($^3\Phi$)	1722.1(933)	1680.6(889)	1685.4(895)	1.0247	1.0218
	506.6(3)	500.8(3)	492.0(2)	1.0116	1.0297
	353.2(0.2)	342.6(0.1)	348.9(0.2)	1.0309	1.0123
	331.8(1)	321.8(2)	327.8(1)	1.0311	1.0122
$NbCO^-$ ($^5\Sigma^+$)	1813.9(987)	1771.1(940)	1773.8(944)	1.0242	1.0226
	433.5(3)	428.3(3)	421.4(2)	1.0121	1.0287
	311.2(16)	301.9(15)	307.2(16)	1.0308	1.0130
$CNbO^-$ (^{3}A′)	888.5(121)	884.7(121)	853.6(106)	1.0043	1.0409
	777.7(64)	753.9(59)	770.4(66)	1.0316	1.0095
	281.9(5)	276.4(4)	275.7(5)	1.0199	1.0225
TaCO ($^6\Sigma^+$)	1893.3(686)	1848.9(650)	1851.0(661)	1.0240	1.0229
	437.9(3)	431.8(4)	424.3(3)	1.0141	1.0321
	304.4(2)	295.3(2)	300.5(2)	1.0308	1.0130
TaCO ($^4\Delta$)	1905.1(637)	1860.5(603)	1862.3(617)	1.0240	1.0230
	443.9(8)	437.7(8)	430.1(7)	1.0142	1.0321
	321.2(0)	311.6(0)	317.1(0)	1.0308	1.0129
CTaO (^{2}A′)	951.9(64)	950.5(66)	904.4(54)	1.0015	1.0525
	739.7(29)	713.6(26)	737.7(31)	1.0366	1.0027
	274.5(1)	269.4(1)	267.5(1)	1.0189	1.0262
CTaO (^{4}A′)	951.1(64)	949.3(67)	905.3(53)	1.0019	1.0506
	807.0(27)	779.0(24)	803.3(31)	1.0359	1.0046
	283.8(1)	278.4(1)	276.8(1)	1.0194	1.0253
Ta[CO] (^{6}A′)	1597.2(304)	1562.1(291)	1557.9(289)	1.0225	1.0252
	476.0(8)	458.5(7)	475.9(8)	1.0382	1.0002
	134.7(4)	134.3(4)	128.1(4)	1.0030	1.0515
$TaCO^-$ ($^3\Phi$)	1687.6(800)	1646.4(765)	1652.5(761)	1.0250	1.0212
	493.6(0.8)	487.2(0.6)	477.4(0.9)	1.0131	1.0339
	349.1(3)	338.5(3)	344.8(3)	1.0313	1.0125
	326.4(0.1)	316.5(0.1)	322.3(0.1)	1.0313	1.0125
$TaCO^-$ ($^5\Sigma^+$)	1782.8(747)	1740.2(717)	1744.0(707)	1.0245	1.0222
	425.1(3)	419.3(3)	411.6(3)	1.0138	1.0328
	231.4(5)	224.4(5)	228.5(5)	1.0312	1.0127
$CTaO^-$ (^{3}A′)	900.6(85)	898.1(89)	858.1(70)	1.0028	1.0495
	726.9(25)	702.0(21)	722.9(30)	1.0354	1.0055
	263.2(5)	258.2(4)	256.7(5)	1.0194	1.0253

Absorptions at 1963.5 and 1984.1 cm^{-1} increase markedly on higher temperature annealing and show carbonyl C−O stretching vibrational frequency ratios. In the mixed experiment, no obvious intermediate components are presented, and these two bands are assigned to the $Nb(CO)_5$ and $Nb(CO)_6$ molecules, respectively.

$Nb(CO)_x^-$. Weak bands are observed in the 1600−1800 cm^{-1} region. These photosensitive bands are reduced to less than 10% of former yield with added CCl_4, which effectively traps ablated electrons, so anion species must be considered.[12−14] The 1768.6 and 1656.7 cm^{-1} bands disappear on $\lambda > 380$ nm photolysis, and give triplet absorptions in the mixed $^{12}C^{16}O+^{12}C^{18}O$ experiment. These two bands are assigned to symmetric and antisymmetric C−O stretching vibrations of the $Nb(CO)_2^-$ anion, which are calculated at 1775.7 and 1686.0 cm^{-1}. The 1713.7 cm^{-1} band destroyed on full-arc photolysis is assigned to the $Nb(CO)_3^-$ anion (C_{3v}) based on quartet mixed isotopic structure, and our BP86 DFT calculation, which predicts 1726.7 and 1824.8 cm^{-1} C−O stretching vibrational frequencies (Table 6). The a_1 mode is much weaker and a 1793.7 cm^{-1} band is probably due to this mode, which shows the same annealing and photolysis behavior as the 1713.7 cm^{-1} band. The 1804.3 cm^{-1} absorption destroyed on full-arc photolysis is tentatively assigned to the $Nb(CO)_4^-$ anion. Finally, there is no evidence for the $NbCO^-$ anion, which is predicted to be less stable than the $CNbO^-$ anion (Table 3).

CNbO. The 919.8, and 783.7 cm^{-1} bands increase markedly on visible photolysis and sharpen together on annealing throughout all of the experiments suggesting different modes of the same molecule. The sharp 919.8 cm^{-1} band shifts to 915.9 cm^{-1} with $^{13}C^{16}O$ and to 883.1 cm^{-1} with $^{12}C^{18}O$, giving a small 12/13 ratio (1.0043) and a large 16/18 ratio (1.0416). On the other hand, the 783.7 cm^{-1} band shifts to 760.2 cm^{-1} with $^{13}C^{16}O$ and to 777.1 cm^{-1} with $^{12}C^{18}O$ giving a contrasting large 12/13 ratio (1.0309) and a small 16/18 ratio (1.0085). The mixed $^{12}C^{16}O+^{13}C^{16}O$ and $^{12}C^{16}O+^{12}C^{18}O$ isotopic spectra clearly

TABLE 5: Geometries, Relative Energies (kcal/mol), Vibrational Frequencies (cm^{-1}), and Intensities Calculated (BP86/D95*/ECP) for OMCCO, $(C_2)MO_2$, $M(CO)_2$, and $M(CO)_2^-$, (M = Nb,Ta)

molecule	relative energy	$(^{12}C^{16}O)_2$	$(^{13}C^{16}O)_2$	$(^{12}C^{18}O)_2$
$Nb(CO)_2$[a]	0	1917.6(483)(*s*-C−O)[i]	1872.4(459)	1875.2(463)
($^4B_2$)		1852.7(1011)(as-C−O)	1809.8(958)	1810.5(975)
ONbCCO[b]	−14.2	2095.4(1457)(C−O)	2031.3(1361)	2070.7(1434)
($^2A'$)		1353.0(44)(CCO)	1314.9(40)	1331.3(36)
		956.3(144)(O−Nb)	956.2(145)	909.8(131)
$(C_2)NbO_2$[c]	+27.8	1766.2(8)(C−C)	1696.7(8)	1766.1(8)
($^2A'$)		957.7(65)(s-ONbO)	957.7(65)	909.7(60)
		916.3(132)(as-ONbO)	916.3(132)	873.5(121)
$Nb(CO)_2^-$ [d]	−31.7	1775.7(1181)(*s*-C−O)	1732.8(1126)	1738.0(1131)
($^3A_2$)		1686.0(934)(as-C−O)	1646.0(886)	1649.0(899)
$Ta(CO)_2$[e]	0	1903.9(513)(*s*-C−O)	1858.5(486)	1862.4(495)
($^4B_2$)		1841.8(1006(as-C−O)	1798.6(953)	1800.7(971)
OTaCCO[f]	−32.6	2112.1(1372)(C−O)	2047.2(1281)	2087.8(1350)
($^2A'$)		1376.6(31)(CCO)	1337.4(34)	1354.7(25)
		960.0(118)(O−Ta)	959.9(119)	909.7(106)
$(C_2)TaO_2$[g]	+6.7	1757.7(13)(C−C)	1688.5(12)	1757.7(13)
($^2A'$)		950.0(28)(s-OTaO)	949.8(28)	899.4(25)
		870.5(67)(as-OTaO)	870.5(67)	825.8(61)
$Ta(CO)_2^-$ [h]	−33.7	1763.5(1372)(*s*-C−O)	1720.8(1304)	1726.2(1318)
($^3A_2$)		1696.2(853)(as-C−O)	1655.1(810)	1660.2(819)

[a] Structure: C_{2v} symmetry, Nb−C: 2.010 Å, C−O: 1.187 Å, ∠CNbC: 87.1°, ∠NbCO: 179.1°. [b] Structure: C_s symmetry, O−Nb: 1.728 Å, Nb−C: 1.922 Å, C−C: 1.324 Å, C−O: 1.192 Å, ∠ONbC: 105.5°. [c] Structure: distorted C_{2v} symmetry, O−Nb: 1.741 Å, Nb−C: 2.193 Å, Nb−C′: 2.520 Å, C−C: 1.284 Å, ∠ONbO: 104.5°, ∠CNbO: 105.7°, ∠C′NbO: 120.8°. [d] Structure: C_{2v} symmetry, Nb−C: 1.966 Å, C−O: 1.217 Å, ∠CNbC: 73.7°, ∠NbCO: 176.8°. [e] Structure: C_{2v} symmetry, Ta−C: 1.987 Å, C−O: 1.191 Å, ∠CTaC: 87.3°, ∠TaCO: 180°. [f] Structure: C_s symmetry, O−Ta: 1.723 Å, Ta−C: 1.913 Å, C−C: 1.322 Å,C−O: 1.190 Å, ∠OTaC: 106.5°. [g] Structure: distorted C_{2v} symmetry, O−Ta: 1.741 Å, Ta−C: 2.147 Å, Ta−C′: 2.484 Å, C−C: 1.286 Å, ∠OTaO: 105.2°, ∠CTaO: 103.5°, ∠C′TaO: 119.3° [h] Structure: C_{2v} symmetry, Ta−C: 1.963 Å, C−O: 1.218 Å, ∠CTaC: 69.8°, ∠TaCO: 178.8°. [i] s: symmetric. as: assymetric.

TABLE 6: Calculated (BP86/D95*/ECP) Geometries, Isotopic C−O Stretching Vibrational Frequencies (cm^{-1}) for $Nb(CO)_3$, $Ta(CO)_3$, $Nb(CO)_3^-$, and $Ta(CO)_3^-$

molecule	relative energy	$(^{12}C^{16}O)_3$	$(^{13}C^{16}O)_3$	$(^{12}C^{18}O)_3$
$Nb(CO)_3$	0	1826.8(1460×2)(e)	1785.8(1378)	1783.2(1415)
($^2A_1$)[a]		1942.7(206)(a_1)	1896.6(196)	1900.0(198)
$Nb(CO)_3$	+10.9	1895.3(741)	1851.5(703)	1851.9(713)
($^4A''$)[b]		1902.7(2044)	1860.0(1934)	1857.3(1976)
		1975.7(152)	1929.5(144)	1931.5(147)
$Nb(CO)_3^-$	−50.4	1726.7(1176×2)(e)	1685.4(1121	1689.4(1124)
($^1A_1$)[c]		1824.8(355)(a_1)	1780.4(340)	1786.6(337)
$Ta(CO)_3$	0	1828.3(1365×2)(e)	1786.3(1290)	1786.2(1322)
($^2A_1$)[d]		1934.6(226)(a_1)	1888.1(214)	1893.1(217)
$Ta(CO)_3$	+6.8	1888.8(756)	1844.6(716)	1846.4(728)
($^4A''$)[e]		1901.0(2108)	1858.2(1994)	1855.8(2039)
		1980.3(111)	1933.3(105)	1936.7(108)
$Ta(CO)_3^-$	−49.7	1725.5(1052×2)(e)	1683.5(1003)	1689.3(1005)
($^1A_1$) [f]		1812.2(445)(a_1)	1767.6(425)	1774.8(425)

[a] Structure: C_{3v} symmtery, Nb−C: 2.014 Å, C−O: 1.186 Å, ∠CNbC: 94.1°. [b] Structure: C_s symmtery, Nb−C(ax): 2.033 Å, C−O: 1.181 Å, Nb−C(eq): 2.120 Å, C−O: 1.178 Å, ∠C(ax)NbC(eq): 88.8°, ∠C(eq)NbC(eq): 148.4°. [c] Structure: C_{3v} symmtery, Nb−C: 1.972 Å, C−O: 1.214 Å, ∠CNbC: 87.3°. [d] Structure: C_{3v} symmtery, Ta−C: 1.993 Å, C−O: 1.189 Å, ∠CTaC: 95.7°. [e] Structure: C_s symmtery, Ta−C(ax): 2.011 Å, C−O: 1.184 Å, Ta−C(eq): 2.100 Å, C−O: 1.178 Å, ∠C(ax)TaC(eq): 89.2°, ∠C(eq)TaC(eq): 156.6°. [f] Structure: C_{3v} symmtery, Ta−C: 1.959 Å, C−O: 1.216 Å, ∠CTaC: 87.3°.

indicate that only one C and one O atom are involved in both modes as only pure isotopic counterparts were observed in mixed isotopic spectra (Figures 6 and 7). Analogous to the NNbO molecule,[11] these bands are assigned to the Nb−O and Nb−C stretching vibrations of the novel CNbO carbide−oxide molecule.

This assignment is strongly supported by DFT calculations which predict a $^2A'$ ground state for CNbO to be 20.4 kcal/mol higher in energy than the NbCO isomer. The Nb−O and Nb−C stretching vibrations are calculated at 930.8 and 822.9 cm^{-1}, which require 0.988 and 0.952 scale factors to match the observed values. These scale factors are slightly smaller than those for a collection of inorganic molecules and comparable calculations.[23] Of more importance, the calculated isotopic ratios (Table 4) characterize normal modes that are primarily Nb−O and Nb−C stretching modes in agreement with observed values. Natural bond orbitals from the DFT calculation suggest the Nb−C and Nb−O both are about 2.5 order with bond lengths 1.826 and 1.744 Å, respectively. The CNbO molecule is polarized: the Mulliken atomic charges are Nb (+0.66), C (−0.26), and O (−0.40). The better match in orbital energies leads to a much more covalent interaction between C and Nb than between Nb and O. The observed Nb−O and Nb−C stretching vibrational frequencies are lower than NbO (978.5 cm^{-1} in neon, 970.6 cm^{-1} in argon matrix)[11,27] and NbC(980 cm^{-1} in gas phase).[28]

$CNbO^-$. The weak absorption at 877.8 cm^{-1} observed after deposition, slightly decreased on 6K annealing, greatly increased on $\lambda > 470$ nm photolysis, but disappeared on $\lambda > 380$ nm photolysis, and failed to return on further annealing. This band

was not found with added CCl_4. All of the above suggest an anion assignment. The 877.8 cm^{-1} band has a 2.8 cm^{-1} carbon-13 isotopic shift and a 37.1 cm^{-1} oxygen-18 shift. No intermediate components were observed in either mixed $^{12}C^{16}O+^{13}C^{16}O$ and $^{12}C^{16}O+^{12}C^{18}O$ experiment, so only one C and O are involved in this mode. The isotopic ratios are very similar to those of the Nb−O stretching mode of the CNbO molecule, while the frequency is 42 cm^{-1} lower; this band is assigned to the Nb−O stretching vibration of the $CNbO^-$ anion. Our DFT calculation predicted $CNbO^-$ with a $^3A'$ ground state and 888.5 and 777.7 cm^{-1} Nb−O and Nb−C stretching vibrational frequencies (121:64 relative intensities); the weaker Nb−C stretching vibration is not observed here. The pronounced growth of $CNbO^-$ on $\lambda > 470$ nm photolysis is accompanied by like growth of CNbO (Figure 2).

ONbCCO. The 2065.5 and 950.9 cm^{-1} bands observed after deposition increased together on photolysis. The 2065.5 cm^{-1} band shifted to 2005.0 cm^{-1} with $^{13}C^{16}O$ and to 2039.7 cm^{-1} with $^{12}C^{18}O$ giving the 12/13 ratio 1.0302 and 16/18 ratio 1.0126. These ratios are significantly larger and smaller, respectively, than diatomic CO ratios, suggesting strong coupling with another C atom. In the mixed $^{12}C^{16}O+^{13}C^{16}O$ experiment, a quartet with approximately 1:1:1:1 relative intensities was produced, while in the mixed $^{12}C^{16}O+^{12}C^{18}O$ experiment only pure isotopic counterparts were presented, suggesting that this is mainly a C−O stretching vibration *coupled* with another inequivalent C atom. The 950.9 cm^{-1} band shows no carbon isotopic shift, but shifted to 904.9 cm^{-1} using $^{12}C^{18}O$ sample; the isotopic 16/18 ratio (1.0508) is very close to the diatomic NbO ratio (1.0511), which indicates that this band is due to a terminal Nb−O stretching vibration. The doublet isotopic structure in the mixed $^{12}C^{16}O+^{12}C^{18}O$ spectrum shows that only one O atom is involved in this mode. These two bands are assigned to the ONbCCO molecule.

Our BP86 calculation predicted that $^2A'$ ground-state ONbCCO is the most stable $Nb(CO)_2$ isomer at this level of theory. The C−O and Nb−O stretching vibrations were calculated at 2095.4 and 956.3 cm^{-1} (scale factors 0.986 and 0.994). Of more importance, the calculated isotopic ratios (12/13: 1.0316, 1.0001 and 16/18: 1.0119, 1.0511) match the experimental values extremely well. The C−CO stretching vibration is predicted at 1353.0 cm^{-1} with lower intensity and is not observed here.

$(C_2)NbO_2$. The 921.6 and 966.2 cm^{-1} bands are produced only on full-arc photolysis. Both bands show no carbon isotopic effect but shift to 879.2 and 918.1 cm^{-1} with $^{12}C^{18}O$. The experimental 16/18 isotopic ratios 1.0490 and 1.0524 are characteristic of antisymmetric and symmetric ONbO vibrations, respectively.[10] In the mixed $^{12}C^{16}O+^{12}C^{18}O$ experiment, triplets with approximately 1/2/1 relative intensities are observed for both bands, which confirms that two equivalent O atoms are involved. These two bands are blue shifted 13.8 and 9.0 cm^{-1} from the ONbO absorptions in neon.[27] The analogous $(O_2)NbO_2$ complex was blue shifted 24.8 and 18.8 cm^{-1} from NbO_2 in solid argon.[10] These two bands are assigned to antisymmetric and symmetric ONbO stretching vibrations of the $(C_2)NbO_2$ complex. Our DFT calculation predicts $(C_2)NbO_2$ to have a $^2A'$ ground state, which is 27.8 and 42.0 kcal/mol higher than the $^4B_2$ $Nb(CO)_2$ and $^2A'$ ONbCCO isomers. The antisymmetric and symmetric ONbO stretching vibrations in $(C_2)NbO_2$ are calculated at 916.3 and 957.7 cm^{-1} with 132:65 relative intensity, which are in excellent agreement with the observed frequencies. The C−C stretching vibration calculated at 1766.2 cm^{-1} with 8 km/mol intensity cannot be observed here.

$Ta(CO)_x$ ($x = 1-6$). The band at 1865.2 cm^{-1} is the major product absorption after Ta deposition using low CO concentration. It increases on annealing, disappears on photolysis, and gives way to a sharp band at 1862.7 cm^{-1} on higher temperature annealing. In the mixed $^{12}C^{16}O+^{13}C^{16}O$ and $^{12}C^{16}O+^{12}C^{18}O$ experiments, both bands exhibit doublet isotopic structure, indicating that only one CO is involved in this mode. These two bands are assigned to the TaCO molecule in different matrix sites, which are compatible with the tentative 1831 cm^{-1} argon matrix assignment.[2] Our DFT calculation found $^6\Sigma^+$ and $^4\Delta$ states very close in energy. As listed in Table 4, the C−O stretching frequencies calculated for both states are very close, but the $^4\Delta$ state value is slightly higher. The calculated isotopic frequency ratios for both states are essentially the same using the BP86 functional, while the B3LYP calculation predicted slightly lower 12/13 and higher 16/18 ratios for both states. Although the calculated frequency for the $^6\Sigma^+$ state fits the experimental value better, the ground state is too close to call, and the ground state could be either $^6\Sigma^+$ or $^4\Delta$. The unusually low observed 12/13 isotopic frequency ratio (1.0219) indicates that both Ta−C and C−O bonds are stretching in this carbonyl mode. There probably are important low-lying configurations not accounted for by DFT calculations for TaCO. Although CASMCSCF calculations have been performed and the $^4\Delta$ ground-state prevails at the highest level,[4] the calculated frequencies are too high to be of diagnostic value owing to the lack of sufficient C and O orbitals in the active space to accurately describe the C−O stretching mode.

The 1838.6 and 1918.3 cm^{-1} bands increased together on annealing, and both bands exhibited carbonyl isotopic ratios (Table 2). In both mixed isotopic experiments, triplets were observed with approximately 1/2/1 relative intensities for both bands (Figure 3) indicating two equivalent CO subunits. These two bands are assigned to the antisymmetric and symmetric C−O stretching vibrations of the $Ta(CO)_2$ molecule, which were calculated at 1841.8 and 1903.9 cm^{-1} in the $^4B_2$ ground state using the BP86 functional. The 1897, 1891 cm^{-1} argon matrix bands tentatively assigned to $Ta(CO)_2$ without benefit of mixed isotopic experiments[2,29] are incorrect; these two bands are most likely the counterparts of 1915.2 and 1900.1 cm^{-1} absorptions in neon, which will be assigned to the $Ta(CO)_4$ molecule.

Our DFT calculations predict a $^2A_1$ ground state with C_{3v} symmetry for $Ta(CO)_3$ with 1828.3 and 1934.6 cm^{-1} antisymmetric and symmetric vibrational frequencies, and no such bands are observed. However, the sharp 1874.6 cm^{-1} band is appropriate for the slightly higher energy C_s structure calculated at 1901.0 cm^{-1} (Table 6), so a tentative assignment is made. The 1916 cm^{-1} argon matrix absorption tentatively assigned to this molecule[2] is probably incorrect.

The 1915.2 and 1900.1 cm^{-1} bands increased together on annealing after the $Ta(CO)_2$ absorptions and are assigned to the $Ta(CO)_4$ molecule, most likely with C_{2v} symmetry. The 1943 cm^{-1} argon matrix band[2] is unlikely to be due to this molecule. The 1954.7 and 1976.0 cm^{-1} absorptions increased markedly on higher temperature annealing, and are assigned to the $Ta(CO)_5$ and $Ta(CO)_6$ molecules, respectively. These are in good agreement with similar 1953 and 1967 cm^{-1} argon matrix bands.

$Ta(CO)_x^-$. Weak bands in the 1800−1700 cm^{-1} region are photosensitive and anion species should be considered. Due to weakness and band overlap, it is difficult to resolve the mixed isotopic structure. On the basis of different photolysis behavior, we tentatively assign the 1700.9 cm^{-1} band to the $TaCO^-$ anion, which was calculated at 1687.6 cm^{-1} in its $^3\Phi$ ground state, the 1773.6 cm^{-1} band to $Ta(CO)_2^-$, the 1716.4 and 1794.3 cm^{-1}

bands to $Ta(CO)_3^-$, and the 1799.5 cm^{-1} band to $Ta(CO)_4^-$, analogous to the Nb+CO system.

OTaCCO. Two bands at 2087.5 and 965.7 cm^{-1} increased markedly on $\lambda > 290$ nm photolysis. The upper band shifted to 2026.2 cm^{-1} with $^{13}C^{16}O$ and to 2061.6 cm^{-1} with $^{12}C^{18}O$ giving a larger 12/13 ratio (1.0302) and a smaller 16/18 ratio (1.0126) compared with diatomic CO. In the mixed $^{12}C^{16}O+^{13}C^{16}O$ experiment, a quartet was produced, while in the mixed $^{12}C^{16}O+^{12}C^{18}O$ experiment only pure isotopic counterparts were present indicating that one O atom and two inequivalent C atoms are involved in this vibrational mode. The associated 965.7 cm^{-1} band showed no carbon isotopic shift but shifted to 915.5 cm^{-1} using $^{12}C^{18}O$ sample; the isotopic 16/18 ratio (1.0548) is just below the calculated harmonic diatomic TaO ratio (1.0553), which indicates that this band is due to a pure terminal Ta−O stretching vibration. The doublet isotopic structure in the mixed $^{12}C^{16}O+^{12}C^{18}O$ spectra confirmed that only one O atom is involved in this mode. These two bands are assigned to the OTaCCO molecule following the ONbCCO example. Our DFT calculation predicted that OTaCCO has a $^2A'$ ground state with bent geometry. The C−O and Ta−O stretching frequencies were calculated at 2112.1 and 960.0 cm^{-1} (scale factors 0.988 and 1.006) with isotopic ratios: (12/13, 1.0317, 1.0001 and 16/18, 1.0116, 1.0553) which are in excellent agreement with experimental values. The C−CO stretching vibration was predicted at 1376.6 cm^{-1} with lower intensity and cannot be observed here.

$(C_2)TaO_2$. The 911.5 cm^{-1} absorption increased markedly on full-arc photolysis. This band showed no shift with $^{13}C^{16}O$ but shifted to 865.2 cm^{-1} with $^{12}C^{18}O$ substitution. The 16/18 ratio (1.0535) is very close to the antisymmetric OTaO ratio (1.0538),[10] while the band position is red-shifted 9.4 cm^{-1} from OTaO in solid neon.[27] The triplet structure in mixed $^{12}C^{16}O+^{12}C^{18}O$ spectra confirms that two equivalent O atoms are involved, and this band is assigned to the $(C_2)TaO_2$ molecule following the $(C_2)NbO_2$ example. The symmetric OTaO vibration is weaker and not observed; however, the mixed $(C_2)^{16}OTa^{18}O$ component was found at 949.5 cm^{-1}, suggesting that this mode for $(C_2)Ta^{16}O_2$ may be covered by the strong OTaCCO absorption at 965.7 cm^{-1}.

Two weaker bands at 884.2 and 864.2 cm^{-1} exhibit similar growth on full-arc photolysis and analogous oxygen-18 substitution; these bands are attributed to higher carbonyl complexes of TaO_2, namely, $(C_2)TaO_2(CO)_x$.

$CTaO^-$. Our DFT calculation predicted the CTaO molecule only about 9.7 kcal/mol (BP86) and 19.1 kcal/mol (B3LYP) higher in energy than the TaCO complex. Although the CNbO molecule is produced in the Nb+CO reaction, no absorption can be assigned to the CTaO molecule. However, a weak band at 902.0 cm^{-1} decreased on annealing and disappeared on $\lambda >$ 290 nm photolysis. This band shifted only 1.7 cm^{-1} with $^{13}C^{16}O$ but exhibited a large (44.3 cm^{-1}) oxygen isotopic shift. The doublet isotopic structure in both mixed experiments confirmed the involvement of only one C and one O atom. This band is assigned to the Ta−O stretching vibration of the $CTaO^-$ anion following the $CNbO^-$ anion identification. Our DFT calculation predicted that the $CTaO^-$ anion is more stable than the $TaCO^-$ anion, although neutral TaCO is more stable than neutral CTaO. The Ta−O and Ta−C stretching vibrations were calculated at 900.6 and 726.9 cm^{-1} with 85:25 relative intensity, but the weaker Ta−C mode is not observed here.

Reaction Mechanisms. The NbCO and TaCO absorptions increased on annealing, particularly TaCO, indicating that ground state (^6D) Nb and Ta (^4F) atoms[30] can react with CO to form monocarbonyls without activation energy, reactions 1. This is also shown by the formation of NbCO using thermal niobium atoms.[3] In fact this major growth of TaCO on annealing by reaction 1b may provide evidence for the $^4\Delta$ ground state. The higher carbonyls were produced and increased on annealing, suggesting that the CO addition reactions 2 can also proceed spontaneously in the cold matrix. Our DFT calculations find $^4B_2$ ground states for both dicarbonyls. There are two spin changes from $^6\Sigma^+$ NbCO to doublet $Nb(CO)_6$ and one spin change from $^4\Delta$ TaCO to doublet $Ta(CO)_6$, but apparently, spin restriction on reactions 2 is not rigorous in the solid matrix. A possible $^4A''$ tee-shaped $Nb(CO)_3$ tricarbonyl was observed, but there was no evidence for the calculated $^2A_1$ pyramidal $Nb(CO)_3$ and $Ta(CO)_3$ ground states.

$$Nb(^6D) + CO(^1\Sigma^+) \rightarrow NbCO(^6\Sigma^+) \quad (1a)$$

$$Ta(^4F) + CO(^1\Sigma^+) \rightarrow TaCO(^4\Delta) \quad (1b)$$

$$NbCO + CO \rightarrow Nb(CO)_2 + CO \rightarrow Nb(CO)_x \ (x = 4,5,6) \quad (2a)$$

$$TaCO + CO \rightarrow Ta(CO)_2 + CO \rightarrow Ta(CO)_x \ (x = 4,5,6) \quad (2b)$$

$$NbCO(^6\Sigma^+) + h\nu \rightarrow Nb[CO]\ (^6A') \rightarrow CNbO\ (^2A') \quad (3)$$

The CNbO absorption increased markedly on visible range photolysis when the NbCO absorption decreased, suggesting that CNbO is formed by photoexcitation of NbCO, reaction 3, which is slightly endothermic. As NbCO is linear, this photoisomization process probably involves a side-bonded intermediate. It is interesting to note that no CTaO product is observed in the Ta+CO system, and the inserted CTaO molecule is calculated to be only 9.7 kcal/mol (BP86) and 19.1 kcal/mol (B3LYP) higher in energy than ground state TaCO. For CNbO and NbCO, this separation is 20.4 kcal/mol with BP86 and 29.1 kcal/mol with B3LYP functionals. As has been mentioned, for both side-bonded Nb[CO] and Ta[CO] only sextet states converged, which are close in energy to the inserted molecules, while both quartet and doublet carbonyl states converged. The ground state of NbCO is a $^6\Sigma^+$ state, so there is no spin restriction to excite NbCO to side-bonded $^6A'$ Nb[CO]. In the case of TaCO, if the ground state is the $^4\Delta$ state, excitation to $^6A'$ is more difficult.

The ONbCCO and OTaCCO molecule absorptions increased markedly on $\lambda > 290$ nm photolysis, when the $Nb(CO)_2$ and $Ta(CO)_2$ absorptions decreased, suggesting that they are formed by rearrangement of the dicarbonyl molecules, reactions 4, which are calculated to be slightly exothermic. Despite the observation of weak NbO and TaO bands, no evidence for CCO was found.[31]

$$Nb(CO)_2 + h\nu \rightarrow ONbCCO \quad (4a)$$

$$Ta(CO)_2 + h\nu \rightarrow OTaCCO \quad (4b)$$

The $(C_2)NbO_2$ and $(C_2)TaO_2$ molecules are produced on full-arc ($\lambda > 240$ nm) photolysis. These molecules are most likely formed by photoinduced rearrangement, reactions 5, which are calculated to be endothermic.

$$ONbCCO + h\nu \rightarrow (C_2)NbO_2 \quad (5a)$$

$$OTaCCO + h\nu \rightarrow (C_2)TaO_2 \quad (5b)$$

Compared to thermal atom reactions, laser ablation produces metal atoms as well as electrons and cations. As a result, anions can be formed via electron capture by neutral molecules and cations can be produced by metal cation reactions. Unfortunately, no metal cation product was observed in these experiments. The $M(CO)_x^-$ and CMO^- anions were observed in the present study along with the common CO^+, $(CO)_2^+$ cations and $(CO)_2^-$ anion.[13,17] The $M(CO)_x^-$ anions are formed by electron capture of neutral molecules, reaction 6, and the CMO^- anions are formed by electron capture or rearrangement reactions 7.

$$M(CO)_x + e^- \rightarrow M(CO)_x^- \quad (6)$$

$$CNbO + e^- \rightarrow CNbO^- \quad (7a)$$

$$TaCO + e^- \rightarrow CTaO^- \quad (7b)$$

Conclusion

Laser-ablated niobium and tantalum atoms have been reacted with CO molecules during condensation in excess neon. The major product $Nb(CO)_x$ and $Ta(CO)_x$ ($x = 1-6$) molecules were formed during sample deposition or on annealing. The novel carbide, oxide molecule CNbO was produced on visible photolysis; however, the analogeous CTaO molecule was not observed. A mechanism of photoinduced isomization of NbCO to CNbO is proposed. In the only other CMO example, which involves uranium, the more stable CUO isomer is observed first and increases on photolysis.[32] The ONbCCO and OTaCCO molecules were also formed via near-UV−visible photon-induced rearrangement of $Nb(CO)_2$ and $Ta(CO)_2$ molecules. The ONbCCO and OTaCCO molecules further rearranged to the $(C_2)NbO_2$ and $(C_2)TaO_2$ molecules on UV photolysis. Evidence is also presented for the $CNbO^-$, $CTaO^-$, $Nb(CO)_x^-$ and $Ta(CO)_x^-$ anions, formed by electron capture of neutral molecules or rearrangement. Density functional theory using core potentials for Nb and Ta atoms has been employed to help identify these products. The calculated vibrational frequencies and isotopic frequency ratios are in good agreement with observed experimental values.

Acknowledgment. We gratefully acknowledge N.S.F. support for this research under Grant CHE 97-00116.

References and Notes

(1) For example, see: (a) Parshall, G. W.; Ittel, S. D. *Homogeneous Catalysis*; Wiley-Interscience: New York, 1992. (b) Bauschlicher, C. W., Jr.; Bagus, P. S.; Nelin, C. J.; Roos, B. O. *J. Chem. Phys.* **1986**, *85*, 345. (c) Basu, P.; Panayotov, D.; Yates, J. T., Jr. *J. Phys. Chem.* **1987**, *90*, 5312. (d) Leung, L. W.; He, J. W.; Goodman, D. W. *J. Chem. Phys*. **1990**, *93*, 8328 and references therein. (e) Lauterbach, J.; Boyle, R. W.; Schick, M.; Mitchell, W. J.; Meng, F.; Weinberg, W. H. *Surf. Sci.* **1996**, *350*, 32. (f) Wovchko, E. A.; Zubkov, T. S.; Yates, J. T., Jr. *J. Phys. Chem. B* **1998**, *102*, 10535.

(2) DeKock, R. L. *Inorg. Chem*. **1971**, *10*, 1205.

(3) Van Zee, R. J.; Weltner, W., Jr. *J. Am. Chem. Soc*. **1989**, *111*, 4519.

(4) Majumdar, D.; Balasubramanian, K. *Chem. Phys. Lett*. **1996**, *262*, 263.

(5) Tan, H.; Liao, M. Z.; Dai, D. G.; Balasubramanian, K. *Chem. Phys. Lett*. **1998**, *297*, 173.

(6) Cox, D. M.; Reichmann, K. C.; Trevor, D. J.; Quilter, A. *J. Chem. Phys*. **1988**, *88*, 111.

(7) Morse, M. D.; Geusic, M. E.; Heath, J. R.; Smalley, R. E. *J. Chem. Phys*. **1985**, *83*, 2293.

(8) Holmgren, L.; Andersson, M.; Rosen, A. *Surf. Sci*. **1995**, *331*, 231.

(9) Severs, M. R.; Chen, Y. M.; Armentrout, P. B. *J. Chem. Phys*. **1996**, *105*, 6322.

(10) Zhou, M. F.; Andrews, L. *J. Phys. Chem. A* **1998**, *102*, 8251 (Nb, Ta+O_2).

(11) Zhou, M. F.; Andrews, L. *J. Phys. Chem. A* **1998**, *102*, 9061; *J. Phys. Chem. A* **1998**, *102*, 10025.

(12) Zhou, M. F.; Andrews, L. *J. Am. Chem. Soc.* **1998**, *120*, 11499 (Ni+CO).

(13) Zhou, M. F.; Chertihin, G. V.; Andrews, L. *J. Chem. Phys*. **1998**, *109*, 10893. Zhou, M. F.; Andrews, L. *J. Chem. Phys.* **1999**, *110*, 10370 (Fe+CO).

(14) Zhou, M. F.; Andrews, L. *J. Phys. Chem. A* **1998**, *102*, 10250; *J. Phys. Chem. A* **1999**, in press (Co, Rh, Ir+CO). Zhou, M. F.; Andrews, L. *J. Am. Chem. Soc*. **1999**. In press.

(15) Burkholder, T. R.; Andrews, L. J. Chem. Phys. **1991**, *95*, 8697.

(16) Hassanzadeh, P.; Andrews, L. *J. Phys. Chem*. **1992**, *96*, 9177.

(17) Thompson, W. E.; Jacox, M. E. *J. Chem. Phys*. **1991**, *95*, 735.

(18) Frisch, M. J.; Trucks, G. W.; Schlegel, H. B.; Gill, P. M. W.; Johnson, B. G.; Robb, M. A.; Cheeseman, J. R.; Keith, T.; Petersson, G. A.; Montgomery, J. A.; Raghavachari, K.; Al-Laham, M. A.; Zakrzewski, V. G.; Ortiz, J. V.; Foresman, J. B.; Cioslowski, J.; Stefanov, B. B.; Nanayakkara, A.; Challacombe, M.; Peng, C. Y.; Ayala, P. Y.; Chen, W.; Wong, M. W.; Andres, J. L.; Replogle, E. S.; Gomperts, R.; Martin, R. L.; Fox, D. J.; Binkley, J. S.; Defrees, D. J.; Baker, J.; Stewart, J. P.; Head-Gordon, M.; Gonzalez, C.; Pople, J. A. *Gaussian 94*, Revision B.1; Gaussian, Inc.: Pittsburgh, PA, 1995.

(19) Perdew, J. P. *Phys. Rev. B* **1986**, *33*, 8822. Becke, A. D. *J. Chem. Phys*. **1993**, *98*, 5648.

(20) Lee, C.; Yang, E.; Parr, R. G. *Phys. Rev. B* **1988**, *37*, 785.

(21) Dunning, T. H., Jr.; Hay, P. J. *Modern Theoretical Chemistry*; Schaefer, H. F., III, Ed. Plenum: NewYork, 1976.

(22) Hay, P. J.; Wadt, W. R. *J. Chem. Phys*. **1985**, *82*, 299.

(23) Bytheway, I.; Wong, M. W. *Chem. Phys. Lett.* **1998**, *282*, 219.

(24) Chertihin, G. V.; Bare, W. D.; Andrews, L. *J. Phys. Chem. A* **1998**, *102*, 3697.

(25) Zhou, M. F.; Andrews, L. *J. Phys. Chem. A* **1999**, *103*, 5259 (V+CO).

(26) Darling, J. H.; Ogden, J. S. *J. Chem. Soc., Dalton Trans*. **1972**, 2496.

(27) Complementary neon matrix experiments were done recently: NbO was observed at 978.5 cm^{-1}, NbO_2 at 957.2(ν_1), 907.8 cm^{-1} (ν_3), NbO_2^- at 931.4 (ν_1), 878.0 cm^{-1} (ν_3) and NbO_3^- at 830.6 cm^{-1}; TaO was observed at 1020.0 cm^{-1}, TaO_2 at 979.2 (ν_1), 920.9 cm^{-1} (ν_3), TaO_2^- at 938.7 (ν_1), 876.6 cm^{-1} (ν_3), and TaO_3^- at 817.3 cm^{-1}.

(28) Simard, B.; Presunka, P. I.; Loock, H. P.; Berces, A.; Launila, O. *J. Chem. Phys*. **1997**, *107*, 307.

(29) The 1819 cm^{-1} argon matrix band, ref 2, may in fact be due to $Ta(CO)_2$, but a mixed isotopic experiment will be required to sustain this possibility.

(30) Moore, C. E. Atomic Energy Levels, Circular 467; National Bureau of Standards, U.S. Department Commerce: Washington, DC, 1949.

(31) Jacox, M. E.; Milligan, D. E.; Moll, N. G.; Thompson, W. E. *J. Chem. Phys.* **1965**, *43*, 3734.

(32) Zhou, M. F.; Andrews, L.; Li, J.; Bursten, B. E. *J. Am. Chem. Soc*. **1999**. In press.